Kinetics and mechanism of gold anode corrosion in a weakly basic aqueous solution of hexamethylenetetramine (urotropine)*

M. D. Vedenyapina,★ S. A. Kulaishin, V. V. Kuznetsov, N. N. Makhova,† and M. M. Kazakova

N. D. Zelinsky Institute of Organic Chemistry, Russian Academy of Sciences,
47 Leninsky prosp., 119991 Moscow, Russian Federation.
E-mail: mvedenyapina@yandex.ru

Electrochemical corrosion of a gold anode in a weakly basic aqueous solution of hexamethylenetetramine (urotropine) was studied in the galvanostatic mode at various currents. The formation of a compact gold deposit as dendrites on the cathode and colloidal gold nanoparticles in the electrolyte was detected by scanning and transmission electron microscopy. The kinetics of anode corrosion was studied by the gravimetric measurements of the loss in weight of the gold anode and the increase in the mass of the cathode over time. By cyclic voltammetry, it was shown that a gold—urotropine complex can be formed at the anode and subsequently migrate to the solution to be reduced at the cathode. After electrolysis, urotropine was isolated from the electrolyte in the unchanged form

Key words: hexamethylenetetramine (urotropine), cyclic voltammetry, gravimetry, Au electrode, corrosion, kinetics, colloidal gold nanoparticles.

The chemistry of gold attracts a lot of attention of researchers because of its ability to form complexes that can be used in various fields of science and technology, such as medicine,[1—7] chemistry of optical materials,[8—10] and catalytic reactions.[11—17] In recent years, high catalytic performance was demonstrated for the synthesized gold complexes with heterocyclic carbenes.[17,18]

As a rule, functional properties of a complex are determined by the nature of the ligand[19,20] present in the coordination sphere of the complexing ion. In particular, gold(III) complexes applicable as anticancer agents and for the therapy of rheumatoid arthritis have been synthesized and extensively studied. A special place is occupied by gold complexes with heterocyclic, cycloaliphatic, and aliphatic diamine derivatives. A new class of cyclometalated gold(III) complexes with benzopyridine, benzylpyridine, and 1,2-diaminocyclohexane (DACH) showed high antiproliferative activity.[20] The Au^{III}—DACH—ethylenediamine complexes, with the DACH amino groups being located in *cis*-, *trans*-, and *S,S*-configurations, showed a cytotoxic activity *in vitro* against the SGC7901 cancer cells; this activity was higher than that of cisplatin.[21] A series of gold(III) complexes with various diamines, including aliphatic α,ω-diaminoalkanes have been synthesized, structurally studied, and assayed for biological activity.[22] Apart from being complexed with aliphatic and cycloaliphatic amino derivatives, gold and other noble metals form complexes with heterocyclic ligands containing donor nitrogen atoms.[23] For example, silver is complexed with pyridine-2,6-dicarboxylate and hexamethylenetetramine (urotropine, HMTA): $Ag(HMTA)_2^{2+}$. Gold complexes with urotropine have not been not reported in the literature.

Studying the electrochemical behavior of structurally diverse aliphatic diamines in weakly basic aqueous solutions with $[K_2CO_3] = 0.05$ mol L^{-1} using gold anode showed that the anode corrodes and then a compact gold deposit is formed on the cathode. In some cases, depending on the type of ligand, nano-sized colloidal gold is formed in the electrolyte solution. The ligands included in the studies were hexahydropyrimidine,[24] 1,5-diazabicyclo[3.1.0]hexane,[24,25] 6-methyl-1,5-diazabicyclo-[3.1.0]hexane,[24,25] 6,6-dimethyl-1,5-diazabicyclo[3.1.0]-hexane,[24,25] 1,3-diaminopropane,[26,27] 2,2-dimethyl-1,3-diaminopropane,[28] ethylenediamine,[27,29] and 1,4-diaminobutane.[30] It is evident that the observed anode corrosion proceeds *via* the formation of gold complexes with the corresponding ligand. Subsequently, these complexes are reduced at the cathode. As this takes place, gold leaves the complex and either forms a compact deposit on the cathode or is released to the electrolyte solution as colloidal nanoparticles.

The goal of this study was to investigate the mechanism and kinetics of corrosion of a gold anode in weakly basic aqueous solutions of hexamethylenetetramine (urotropine), which is accompanied by the formation of a gold deposit on the cathode and nanosized colloidal gold.

* Dedicated to Academician of the Russian Academy of Sciences O. M. Nefedov on the occasion of his 90th birthday.
† Deceased

Published in Russian in *Izvestiya Akademii Nauk. Seriya Khimicheskaya,* No. 1, pp. 52—58, January, 2022.

Results and Discussion

For more comprehensive study of the mechanism and kinetics of gold anode corrosion, the electrolysis was carried out at four currents (1, 5, 10, and 20 mA) for 40 h. In line with our earlier results,[24–31] the Au anode corroded thus losing weight. Simultaneously, gold metal was deposited on the steel cathode. Figure 1 shows the time dependences of the weight loss of the gold anode (m_{corr}), the weight gain of the cathodic deposit (m_{dep}), and the weight of gold (m_{sol}) located in the working solution, which is calculated as the difference of the former two values, for various currents of electrolysis. It can be seen that during electrolysis, the dependences $m_{corr} = f(t)$ are linear for any of the currents, except for 1 mA. The curve recorded for 1 mA (see Fig. 1, *a*) attests to the existence of a considerable induction effect. Analysis of the dependences $m_{corr} = f(t)$ showed that the loss in weight of the gold anode starts only 20 h after the beginning of electrolysis. The increase in the weight of the cathode deposit and the amount of gold in the electrolyte solution (m_{dep} and m_{sol}) with increasing time of electrolysis is nonlinear. The dependence $m_{dep} = f(t)$ for 1 and 5 mA currents (see Fig. 1, *a* and *b*) also shows an induction effect of the cathodic process. At 10 and 20 mA currents (see Fig. 1, *c* and *d*), the m_{sol} value does not exceed 6 mg. Obviously, in the beginning of the electrolysis, the gold deposition on the cathode is retarded due to the insufficient metal concentration in the solution (see Fig. 1, *a*). Apparently, a certain amount of gold should appear in the solution before it can be deposited on the cathode (see Fig. 1, *d*).

Figure 2 shows the dependence of the calculated weight of gold in the solution m_{sol} (Fig. 2, *a*) and the weight of the cathodic gold deposit m_{dep} (Fig. 2, *b*) on the current of

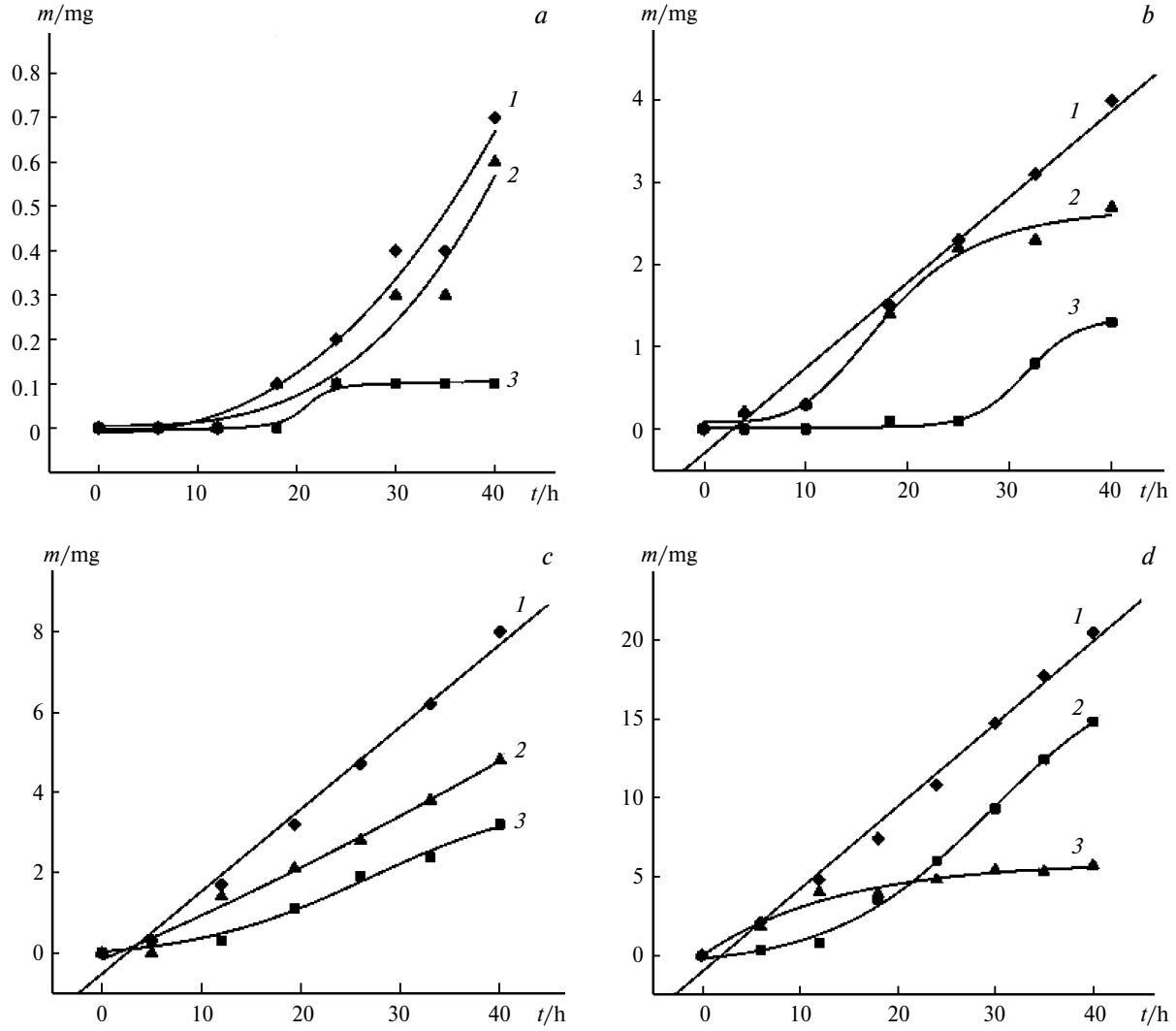

Fig. 1. Time dependences of the anodic dissolution and cathodic deposition of gold in a weakly basic aqueous solution of urotropine (C = 1.0 mol L^{-1}) at various currents: 1 (*a*), 5 (*b*), 10 (*c*), and 20 mA (*d*); (*1*) weight loss of gold anode (m_{corr}), (*2*) calculated weight of gold present in the solution (m_{sol}), (*3*) weight of the gold metal deposit formed on the steel cathode (m_{dep}).

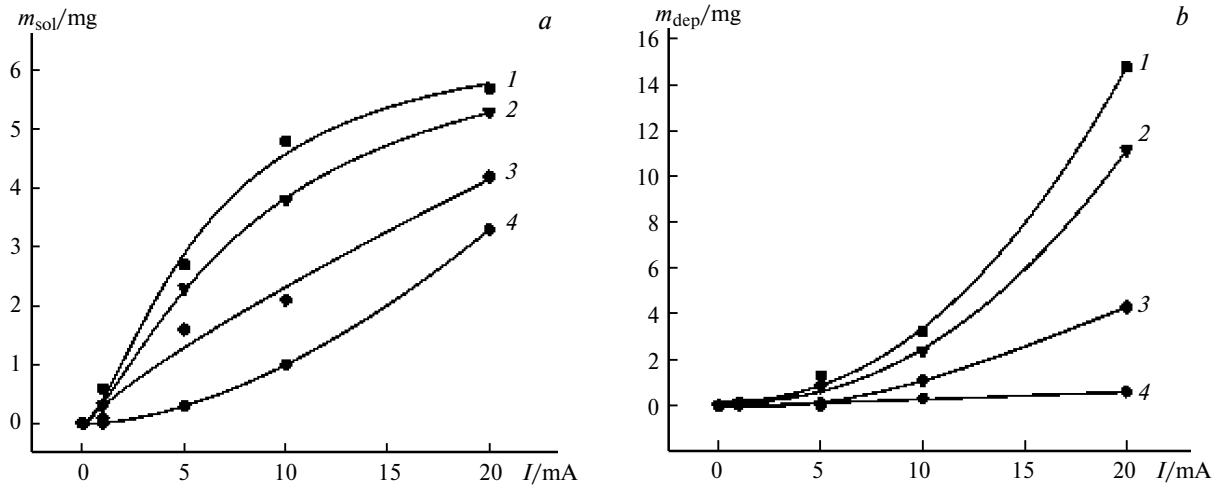

Fig. 2. Calculated amount of gold in the solution (m_{sol}) (*a*) and the weight of the gold deposit on the cathode (m_{dep}) (*b*) *vs.* current of electrolysis in a weakly basic aqueous solution of urotropine, I/mA: 20 (*1*), 10 (*2*), 5 (*3*), and 1 (*4*); time of electrolysis: 40 h, $C_0 = 1.0$ mol L^{-1}.

electrolysis. Analysis of the dependences shown in Fig. 2 made it possible to select the optimal conditions for preparative electrolysis providing the highest gold content in the solution: the current of electrolysis should be above 10 mA, the urotropine concentration $C_0 = 1.0$ mol L^{-1}, and the electrolysis time should be 40 h.

By analogy with previous studies,[24—31] the observed kinetics of the anodic dissolution and cathodic deposition of gold can be analyzed using a system of differential equations:

$$dm_1/dt = k_1, \quad (1)$$

$$dm_2/dt = k_1 - k_2 m_2, \quad (2)$$

$$dm_3/dt = k_2 m_2, \quad (3)$$

where m_1, m_2, and m_3 are the weights of gold that migrates from the anode to the solution, is deposited on the cathode from the solution, and is located in the solution at time t, respectively. Solving this system of equations by means of the Mathcad software gave the k_1 and k_2 values that most accurately described the experimental results shown in Fig. 1. The k_1 and k_2 values for the corrosion of gold anode at various currents are summarized in Table 1.

The studies showed that the rate constant for the cathodic deposition of gold (k_2) is maximum when corrosion is conducted at a current of 10 mA using a steel cathode (see Table 1). This confirmed the conclusion that under these conditions, the current of electrolysis of 10 mA is most efficient for gold migration from the anode to the cathode in a weakly basic aqueous solution of urotropine.

Cyclic voltammetry (CV) curves for the gold electrode in a weakly basic aqueous solution of urotropine measured in the potential range from 0 to +1200 mV at various potential scan rates are shown in Fig. 3.

The anodic branches of CV curves exhibit peaks at the potentials $E = 600$—1000 mV. It was found that the peak currents $I_{p,a}$ increase with increasing potential scan rate v. Their shifts towards more positive potentials can be seen. In the measurements of several CV cycles, responses in the anodic and cathodic CV branches are observed in the first and the last cycles. This attests to the absence of a strong substrate adsorption that would passivate the anode surface. When reverse scanning is carried out in the potential range $E = 0$—400 mV, the cathodic branches show peaks, indicating the reduction of the corrosion products. The cathodic peak currents ($I_{p,c}$) depend linearly on the potential scan rate (see Fig. 3), which indicates that Au corrosion products are reduced directly on the electrode surface. Hence, the electrochemical reaction is rate-limited by the electron transfer. In this case, the Laviron equation is applicable:[32]

$$I_p = nFQ_v/4RT,$$

where n is the number of electrons participating in the reaction per molecule, F is the Faraday number, amount-

Table 1. Kinetic characteristics of the corrosion of gold anode in a weakly basic aqueous solution of urotropine

I/mA	Cathode	k_1/mg h^{-1}	k_2/h^{-1}	Dissolution rate /mg cm^{-2} h^{-1}
1	Steel	0.017	0.007	0.29
5	Steel	0.10	0.016	1.59
10	Steel	0.25	0.020	3.96
20	Steel	0.51	0.014	8.09
10	Platinum	0.22	0.018	3.49

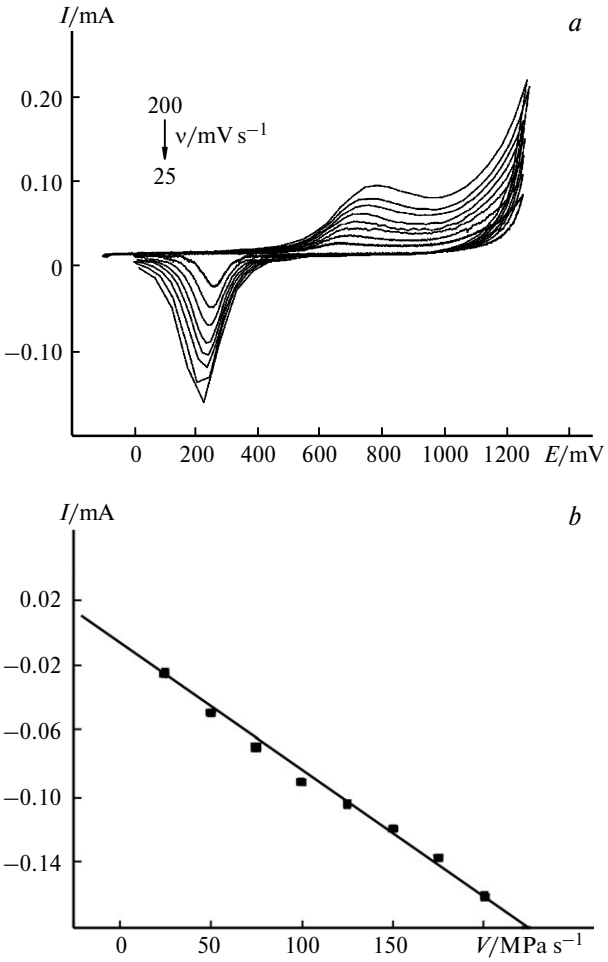

Fig. 3. Cyclic voltammograms in a weakly basic aqueous solution (0.05 *M* K_2CO_3) of urotropine on the Au electrode at various potential scan rates: 200, 175, 150, 125, 100, 75, 50, and 25 mV s^{-1} (*a*) and dependence of the cathodic peak current on the potential scan rate according to CV data (*b*).

ing to 96485 C mol^{-1}; Q is the charge corresponding to the peak area in the cathodic branch; v is the potential scan rate, mV s^{-1}; R is the gas constant, amounting to 8.314 J mol^{-1} K^{-1}; and T is the absolute temperature, K.

Using this equation, it was found that in the range v = 25—200 mV s^{-1}, the reaction involves 1.7—2.2 electrons. Thus, it can be taken that, on average, two electrons participate in the cathodic reduction of corrosion products in a weakly basic aqueous solution of urotropine. The anodic peak currents ($I_{p,a}$) increase with increasing scanning rate of the potential v and linearly depend on $v^{0.5}$. This indicates that diffusion of the dissolved substrate to the electrode is the rate-limiting step.

The results of scanning electron microscopy and energy dispersive X-ray spectroscopy studies of the steel cathode surface are shown in Fig. 4. The results indiicate that during the corrosion of the gold anode, dendrite-like Au deposit appears on the surface of the steel cathode (see Fig. 4).

During the gold anode corrosion at any of the currents (5, 10, or 20 mA), the weakly basic aqueous solution of urotropine acquired a light violet color, and after 40 h of electrolysis, the electrolyte solution color became more intense. A TEM examination of the working solution revealed colloidal gold particles in all cases (Fig. 5).

The colloidal gold particles formed at 20 mA are much smaller in size (3—7 nm) and greater in number than the particles formed at 5 or 10 mA (5—10 nm).

It has been shown previously that during electrolysis in the presence of aliphatic diamines, gold migrates from the anode to the cathode through the intermediate formation of a complex with a ligand; this complex is reduced at the cathode to give not only gold as a cathodic deposit or a colloid, but also the initial ligand or its derivatives. Therefore, it was of interest to find out whether any gold complexes with urotropine or some ligand transformation

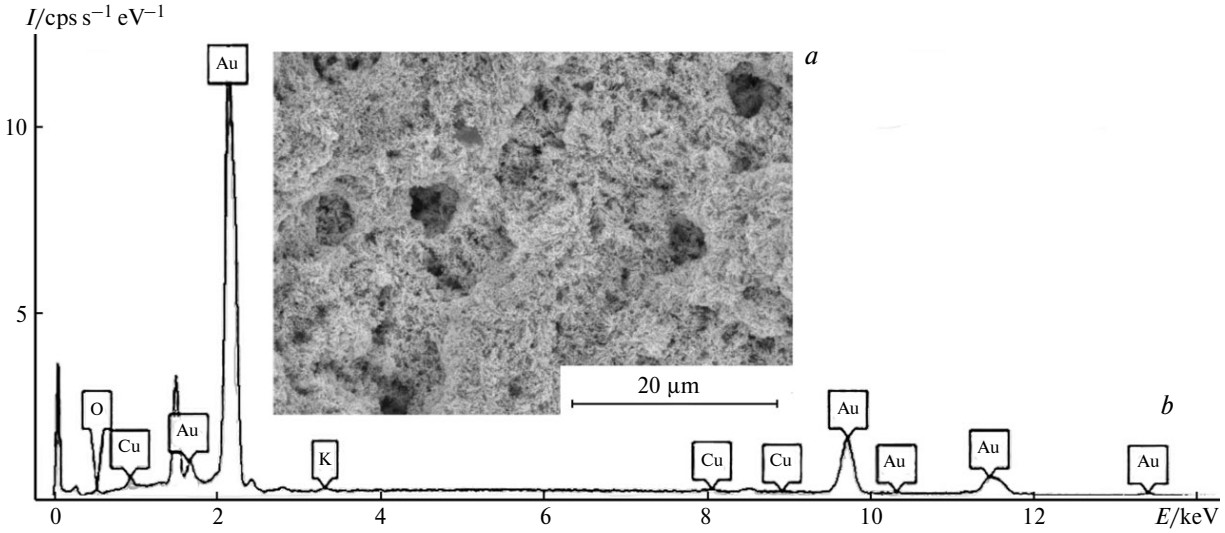

Fig. 4. Electron microscopic image (*a*) and results of EDX study of the chemical composition (*b*) of the steel cathode surface.

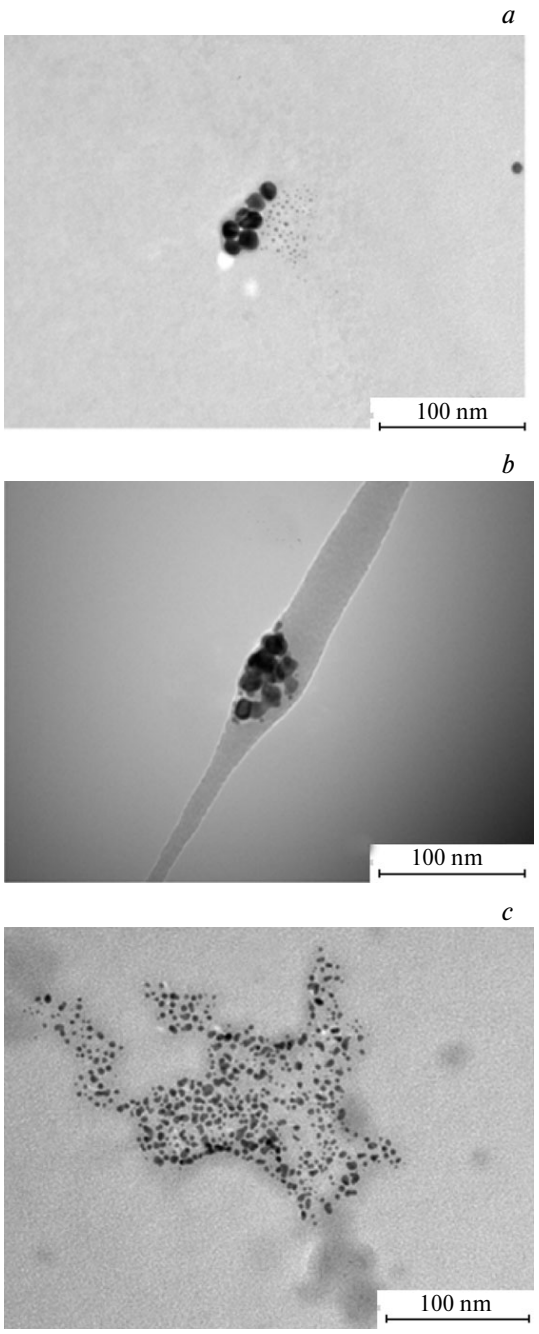

Fig. 5. Electron microscopic image of the colloidal gold particles in the electrolyte medium 40 h after the electrolysis at a current of 5 (*a*), 10 (*b*), and 20 mA (*c*).

products are formed during the processes studied here. Therefore, after completion of the electrolysis, the reaction solution was allowed to stand in an open glass crystallizing dish at room temperature until water completely evaporated, and then the organic component was extracted from the residue with methanol. Contrary to expectations, only pure urotropine was present in the extract, according to the results of physicochemical methods (IR and ^{1}H, ^{13}C NMR spectra). No complexes of urotropine with gold were found in the solution. Evidently, gold complexes with urotropine were unstable and were completely reduced at the cathode. Since electrolysis was carried out in a 0.05 *M* aqueous solution of K_2CO_3, while urotropine is hydrolyzed only in acid media, complexes have apparently formed only with pure urotropine.

Thus, the kinetics and mechanism of anode corrosion of gold under galvanostatic conditions in a weakly basic aqueous solution of hexamethylenetetramine (urotropine) were studied for the first time. The formation of a gold—urotropine complex was revealed by cyclic voltammetry and gravimetry. The complex is reduced at the cathode to give a cathodic deposit and colloidal gold in the electrolyte medium. A morphological TEM study of the Au anode demonstrated the formation of different nano-sized structures of colloidal gold, depending on the electrolysis current, 1, 5, 10, or 20 mA. A large number of smaller nanoparticles was observed at 20 mA. The process kinetics was investigated by gravimetric analysis. It is obvious that urotropine takes part in the complex formation in the pristine form, since it is recovered unchanged from the electrolyte after the electrolysis. This study is the first example of electrochemical generation of a gold complex with a polyheterocyclic nitrogen-containing cage molecule.

Experimental

Commercial ACROS urotropine was used. The working solutions were prepared using doubly distilled water. K_2CO_3 was of analytically pure grade. The anodic corrosion of gold was studied by carrying out electrolysis under galvanostatic conditions in an undivided two-electrode cell. Gold and steel or platinum wires 0.3 mm in diameter immersed into an electrolyte solution to 15 mm served as the anode and the cathode, respectively. The urotropine concentration in a 0.05 *M* solution of K_2CO_3 was 1.0 mol L^{-1}, the working solution volume was 20 mL. The electrodes were weighed on an ABJ220-4NM electronic analytical balance (Kern, USA) (d = 0.0001 g) at certain time intervals for 40 h.

Cyclic voltammograms were recorded using a computer-controlled IPC Compact potentiostat in a three-electrode cell. A gold wire (99.99% Au) of 0.3 mm in diameter and 0.3 cm in length sealed into glass was used as the working electrode. A steel wire of the same size sealed into glass was the auxiliary electrode, and a silver chloride reference electrode (Ag/AgCl/3*M* KCl) was used. A 0.05 *M* solution of K_2CO_3 with pH 11.1 served as the supporting electrolyte. The urotropine concentration was 0.1 mol L^{-1}. In the CV measurements, the potential sweep rates (v) were 200, 175, 150, 125, 100, 75, 50, and 25 mV s^{-1}.

The microstructure of the electrodes obtained after the gold electrolysis in the aqueous solution of urotropine was studied by field emission scanning electron microscopy (FE-STEM) on a Hitachi SU8000 electron microscope (Hitachi, Japan). The images were taken in the secondary electron mode at an accelerating voltage of 2—30 kV and a working distance of 8.4—11.0 mm. The analytical measurements were optimized by a previously described approach.[33—34] The energy dispersive X-ray spectroscopy (EDX) studies were carried out on an Oxford Instruments

X-max energy dispersive spectrometer (UK). The electrodes (gold and steel wires) were investigated by placing them on an aluminum stage 25 mm in diameter and fixing with two screws. The electrolyte obtained after the electrolysis and containing colloidal gold was examined by transmission electron microscopy (TEM) on a Hitachi HT7700 electron microscope (Japan). The images were taken in the transmission electron mode (bright field mode) at an accelerating voltage of 100 kV. Before the measurements, the working solution was deposited onto a thin carbon film attached to a copper grid with a diameter of 3 mm, which was fixed in a special holder. The sample was deposited in the liquid state and then dried *in vacuo*.

The product formed after electrolysis was isolated by keeping the reaction solution in an open glass crystallizing dish at room temperature until water completely evaporated. The resulting solid residue was extracted with methanol (2×50 mL) and then the solvent was evaporated *in vacuo*. The IR spectra of the starting urotropine and the product isolated by methanol extraction were measured on a Bruker Alpha spectrometer in the 400—4000 cm^{-1} range. The ^1H and ^{13}C NMR spectra of the starting urotropine and the product isolated by methanol extraction were recorded in D_2O on a Bruker AM-300 spectrometer (300 MHz for ^1H and 75.5 MHz for ^{13}C). The ^1H NMR chemical shifts were referred to the residual protons of D_2O. The ^{13}C NMR spectra of the solvent were recorded using tetramethylsilyl propionate (TSP) as the chemical shift standard. All spectra of the initial urotropine and the product isolated by methanol extraction fully coincided both with each other and with published data (^1H NMR (D_2O), δ: 4.74 (s); ^{13}C NMR (D_2O, TSP): δ = 73.0;[35] IR, ν/cm^{-1}: 2993, 2953, 2922, 2872, 2655, 1458, 1440, 1371, 1239, 1048, 1012, 812, 672, 512.

The authors are grateful to the Department of Structural Studies of the N. D. Zelinsky Institute of Organic Chemistry, Russian Academy of Sciences, for electron microscopy examination of the samples.

No human or animal subjects were used in this study.

The authors declare no competing interests.

References

1. P. I. d. S. Maia, V. M. Deflon, U. Abram, *Future Med. Chem.*, 2014, **6**, 1515; DOI: 10.4155/fmc.14.87.
2. I. Ott, *Coord. Chem. Rev.*, 2009, **253**, 1670; DOI: 10.1016/j.ccr.2009.02.019.
3. H. Goitia, Y. Nieto, M. D. Villacampa, C. Kasper, A. Laguna, M. C. Gimeno, *Organometallics*, 2013, **32**, 6069; DOI: 10.1021/om400633z.
4. B. Bertrand, A. Casini, *Dalton Trans.*, 2014, **43,** 4209; DOI: 10.1039/C3DT52524D.
5. T. Zou, C. T. Lum, C.-N. Lok, J.-J. Zhang, C.-M. Che, *Chem. Soc. Rev.*, 2015, **44,** 8786; DOI: 10.1039/C5CS00132C.
6. R. Visbal, V. Fernández-Moreira, I. Marzo, A. Laguna, M. C. Gimeno, *Dalton Trans.*, 2016, **45**, 15026; DOI: 10.1039/C6DT02878K.
7. C. Yeo, K. Ooi, E. Tiekink, *Molecules*, 2018, **23**, 1410; DOI: 10.3390/molecules23061410.
8. O. Crespo, M. C. Gimeno, P. G. Jones, A. Laguna, J. M. López-de-Luzuriaga, M. Monge, J. L. Pérez, M. A. Ramón, *Inorg. Chem.*, 2003, **42**, 2061; DOI: 10.1021/ic0259843.
9. O. Crespo, M. C. Gimeno, A. Laguna, C. Larraz, M. D. Villacampa, *Chem.—Eur. J.*, 2006, **13**, 235; DOI: 10.1002/chem.200600566.
10. R. Czerwieniec, T. Hofbeck, O. Crespo, A. Laguna, M. C. Gimeno, H. Yersin, *Inorg. Chem.*, 2010, **49**, 3764; DOI: 10.1021/ic902325n.
11. A. S. K. Hashmi, G. J. Hutchings, *Angew. Chem., Int. Ed.*, 2006, **45**, 7896; DOI: 10.1002/anie.200602454.
12. A. S. K. Hashmi, *Chem. Rev.*, 2007, **107**, 3180; DOI: 10.1021/cr000436x.
13. A. Fürstner, P. W. Davies, *Angew. Chem., Int. Ed.*, 2007, **46,** 3410; DOI: 10.1002/anie.200604335.
14. Z. Li, Brouwer, C. He, *Chem. Rev.*, 2008, **108**, 3239; DOI: 10.1021/cr068434l.
15. D. Garayalde, C. Nevado, *Beilstein J. Org. Chem.*, 2011, **7**, 767; DOI: 10.3762/bjoc.7.87.
16. M. Rudolph, A. S. K. Hashmi, *Chem. Soc. Rev.*, 2012, **41,** 2448; DOI: 10.1039/C1CS15279C.
17. I. J. B. Lin, C. S. Vasam, *Can. J. Chem.*, 2005, **83**, 812; DOI: 10.1139/v05-087.
18. M. Aliaga-Lavrijsen, R. P. Herrera, M. D. Villacampa, M. C.n Gimeno, *ASC Omega*, 2018, **3**, 9805; DOI: 10.1021/acsomega.8b01352.
19. D. J. Gorin, B. D. Sherry, F. D. Toste, *Chem. Rev.*, 2008, **108**, 3351; DOI: 10.1021/cr068430g.
20. S. Gukathasan, S. Parkin, S. G. Awuah, *Inorg. Chem.*, 2019, **58**, 9326; DOI: 10.1021/acs.inorgchem.9b01031.
21. S. S. Al-Jaroudi, M. Monim-ul-Mehboob, M. Altaf, A. A. Al-Saadi, M. I. M. Wazeer, S. Altuwaijri, A. A. Isab, *Biometals*, 2014, **27**, 1115; DOI: 10.1007/s10534-014-9771-2.
22. B. Petrovic, S. Radisavljevic, *Front. Chem.*, 2020, **8**, 379; DOI: 10.3389/fchem.2020.00379.
23. L. V. Antonova, T. E. Busygina, *Vestn. Tekhnol. Un-ta* [*Bull. Technol. Univ.*], 2016, **19**, 5 (in Russian).
24. A. P. Simakova, M. D. Vedenyapina, V. V. Kuznetsov, N. N. Makhova, A. A. Vedenyapin, *Russ. J. Phys. Chem. A*, 2014, **88**, 331; DOI: 10.1134/S0036024414020241.
25. M. D. Vedenyapina, V. V. Kuznetsov, N. N. Makhova, A. A. Vedenyapin, *Russ. J. Phys. Chem. A*, 2016, **90**, 1903; DOI: 10.1134/S0036024416090284.
26. M. D. Vedenyapina, G. Ts. Ubushieva, V. V. Kuznetsov, N. N. Makhova, A. A. Vedenyapin, *Russ. J. Phys. Chem. A*, 2016, **90**, 2312; DOI: 10.1134/S0036024416110297.
27. M. D. Vedenyapina, V. V. Kuznetsov, D. I. Rodikova, N. N. Makhova, A. A. Vedenyapin, *Mendeleev Commun.*, 2018, **28**, 181; DOI: 10.1016/j.mencom.2018.03.024.
28. M. D. Vedenyapina, V. V. Kuznetsov, N. N. Makhova, D. I. Rodikova, *Russ. Chem. Bull.*, 2020, **69**, 1884; DOI: 10.1007/s11172-020-2974-5.
29. M. D. Vedenyapina, V. V. Kuznetzov, A S. Dmitrenok, M. E. Minyaev, N. N. Makhova, M. M. Kazakova, *Russ. Chem. Bull.*, 2021, **70**, 735; DOI: 10.1007/s11172-021-3144-0.
30. M. D. Vedenyapina, V. V. Kuznetsov, N. N. Makhova, D. I. Rodikova, *Russ. J. Phys. Chem. A*, 2019, **93**, 466; DOI: 10.1134/S0036024419020304.

31. M. D. Vedenyapina, V. V. Kuznetsov, N. N. Makhova, D. I. Rodikova, *Russ. Chem.Bull.*, 2019, **68**, 1997; DOI: 10.1007/s11172-019-2658-1.
32. E. J. Laviron, *Electroanal. Chem. Interf. Electrochem.*, 1979, **101**, 19; DOI: 10.1016/S0022-0728(79)80075-3.
33. V. V. Kachala, L. L. Khemchyan, A. S. Kashin, N. V. Orlov, A. A. Grachev, S. S. Zalesskiy, V. P. Ananikov, *Russ. Chem. Rev.*, 2013, **82**, 648; DOI: 10.1070/RC2013v082n07ABEH004413.
34. A. S. Kashin, V. P. Ananikov, *Russ. Chem. Bull.*, 2011, **60**, 2602; DOI: 10.1007/s11172-011-0399-x.
35. Y. Shen, S. Hue, Y. Zhao, Q. Zhu, Z. Tao, *Chin. Sci. Bull.*, 2003, **48**, 2694; DOI: 10.1007/BF02901758.

Received May 28, 2021;
in revised form June 22, 2021;
accepted July 21, 2021